Detection of DNA mutations using a capacitive micro-membrane array

Vasiliki Tsouti[a,*], Christos Boutopoulos[b], Peristera Andreakou[b], Marina Ioannou[c],
Ioanna Zergioti[b], Dimitris Goustouridis[a], Dimitris Kafetzopoulos[c], Dimitris Tsoukalas[b],
Pascal Normand[a], Stavros Chatzandroulis[a]

[a] Institute of Microelectronics NCSR Demokritos, Terma Patriarchou Grigoriou, Aghia Paraskevi, 15310 Athens, Greece
[b] Department of Applied Sciences, National Technical University of Athens, Zografou 15780, Greece
[c] Institute of Molecular Biology and Biotechnology FORTH, Heraklion, Greece

A B S T R A C T

The detection of DNA hybridization using capacitive readout and a biosensor array of ultrathin Si membranes is presented. The biosensor exploits the ability of the ultrathin membranes to deflect upon surface stress variations caused by biological interactions. Probe DNA molecules are immobilized on the membrane surface and the surface stress variations during hybridization with their complementary strands force the membrane to deflect and effectively change the capacitance between the flexible membrane and the fixed substrate. The sensor array comprises 256 such sensing sites thus allowing the concurrent sensing of multiple DNA mutations. The biosensor and its performance for the detection of complementary DNA strands are demonstrated using beta-thalassemia oligonucleotides. The experimental results show that the presented sensors are able to detect DNA hybridization and to discriminate single nucleotide mismatches.

© 2010 Elsevier B.V. All rights reserved.

1. Introduction

The detection of different DNA mutations in a fast and easy way is increasingly important in disease screening. Typical analysis with microarrays serves the fast and easy genome analysis through the use of labels (Shiu and Borevitz, 2008). However, among the limitations of this technology is that expensive and bulky systems are required in order to measure the label signal (Chen and Sullivan, 2003). These limitations hinder the miniaturization of typical microarrays and thus their use in point of care diagnostics. In addition, labelling is a time and cost consuming process and may affect the interaction between the probe and target molecules. In order to address these issues, miniaturized and label-free systems such as electrical biosensors and surface stress based biosensors have emerged. The electrical biosensors can be amperometric, voltametric, impedance or capacitive sensors (Daniels and Pourmand, 2007; Berggren et al., 2001). Surface stress based biosensors are usually bimorph microcantilevers with optical or piezoresistive readout (Fritz, 2008) or alternatively capacitive micro-membranes (Cha et al., 2008; Tsouti et al., 2009).

Electrical readout features low power consumption and high miniaturization potential. In addition, the capability of label-free sensing allows for significant gains in the time and cost required for sample preparation. Another advantage of these systems is that the biological interactions can be monitored in real time. Real-time measurements may give additional information regarding the samples, as well as enable studying the kinetics of the interactions, understanding the physical processes taking place, and consequently optimizing the sensor performance (Peterson et al., 2001; Dai et al., 2002; Bhanot et al., 2003). A limitation of electrical biosensors is the low density of sensing sites compared to typical microarrays. Electrical microarrays accommodating up to a few tens or hundreds of sensing elements have been presented (Guiducci et al., 2006; Benini et al., 2007; Levine et al., 2009). However, in some microarrays signal amplification schemes seem to be necessary for effective sensing (Mehta et al., 2007).

Surface stress based biosensors require flexible structures, microcantilevers or membranes, where one of their surfaces is functionalized with the probe biomolecules. The interaction with the appropriate target molecules induces surface stress variations and finally changes in the deflection of the structure. Microcantilever biosensors provide high sensitivity and the ability of parallelization into arrays for simultaneous multiple sensing through the use of differently functionalized cantilevers. In most cases, cantilever bending is detected optically (Fritz et al., 2000; Hansen et al., 2001; Zhang et al., 2006) or by utilizing the piezoresistive effect (Mukhopadhyay et al., 2005). Optical detection however, is difficult to miniaturize as it requires costly and cumbersome setups, and is also not easily applied in opaque liquids such as blood. On the other hand, piezoresistive detection may result

in thermal drift. Capacitive detection is desirable as it is highly sensitive and requires low power consumption but is not feasible in cantilever biosensors as the electrolyte solution causes faradaic currents between the capacitor plates. When a membrane is used instead of a cantilever, the capacitor plates are sealed from the electrolyte solution thereby enabling reliable capacitive detection.

Capacitive membranes, similarly to cantilevers, exploit the variations of the surface stress induced when the probe molecules on the functionalized surface interact with their target counterparts. The sensing element of a capacitive membrane biosensor consists of a rigid fixed electrode implemented on the substrate, a cavity and the flexible membrane electrode overhanging the cavity. The probe molecules are immobilized on the membrane surface and upon interaction with the appropriate target molecules, the membrane deflects due to surface stress variations. The deflection is translated into a change in capacitance between the flexible electrode and the substrate.

A successful biological application of capacitive membranes made of 2–4 μm thick polydimethylsiloxane (PDMS) has been presented by Cha et al. (2008). These membranes are covered by a thin gold layer serving the immobilization of probe molecules. The detection of DNA hybridization and protein recognition by aptamers are demonstrated. The capacitance variations for the hybridization of 16-mer oligonucleotides in concentration 1 μM in 1 M PBS solution were about 6 fF for square membranes with 500 μm side length and 2 μm thickness.

Similar efforts to fabricate capacitive surface stress based biosensors without demonstrating at the moment applications for the detection of particular biological interactions have also emerged. Satyanarayana et al. (2006) present a parylene micromembrane surface stress sensor and demonstrate its response in chemical sensing. The accomplishment of more effective chemical and potentially biological sensing through a membrane closer to its substrate is discussed by Sivaramakrishnan et al. (2008), where electret membranes have been exploited. Another alternative of capacitive membranes for biological sensing could be the capacitive micromachined ultrasonic transducer (CMUT) example, also demonstrated in chemical sensing (Park et al., 2007). These are mass sensitive devices and in particular an array of vacuum-backed resonating membranes connected in parallel. The surface of the membranes is covered by the sensing layer and during the interaction with the appropriate analyte the elements' mass increases and a shift on their oscillation frequencies is observed. Although these devices perform very well in chemical sensing, their application on biological sensing is not reported yet.

In the present work, the capacitive sensing elements are parts of a 2D array (16 × 16) and are composed of an ultrathin silicon membrane passivated by a low temperature oxide (LTO) layer that also serves for the functionalization of the biosensors. The sensor array fabrication and its response to the detection of protein interactions have been presented by Tsouti et al. (2008, 2009). The evaluation of the devices for effective DNA sensing is presented in the following sections.

2. Experimental

2.1. Sensor array description

The capacitive biosensor incorporates an array of 16 × 16 sensing elements that occupy an area of 5 mm × 5 mm. Therefore, the array can accommodate up to 256 differently functionalized sensing elements in a small area. The operation principle of the sensors relies on the membrane deflection capability and the translation of the deflection changes into capacitance changes. The basic capaci-
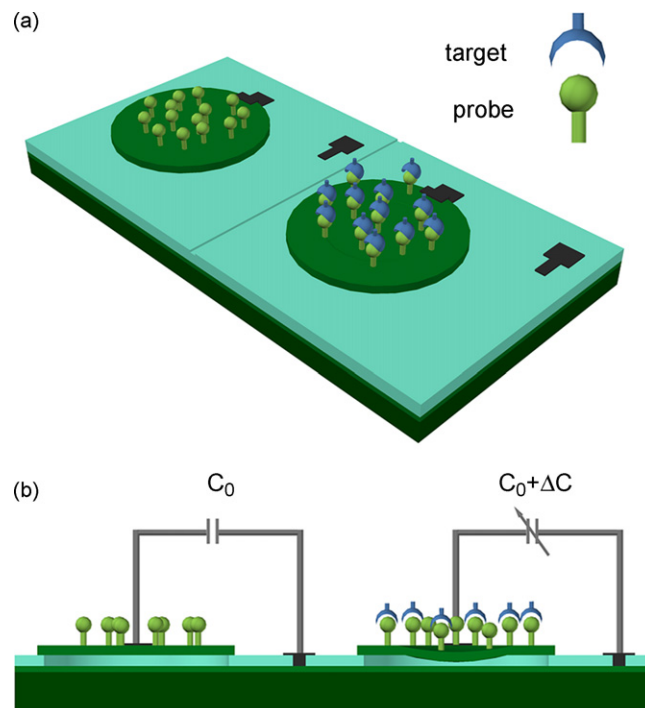
Fig. 1. Schematic of the capacitive sensing elements. The surface stress variations induced during the biomolecular interactions change the capacitance between the ultrathin Si membranes and the fixed substrate.
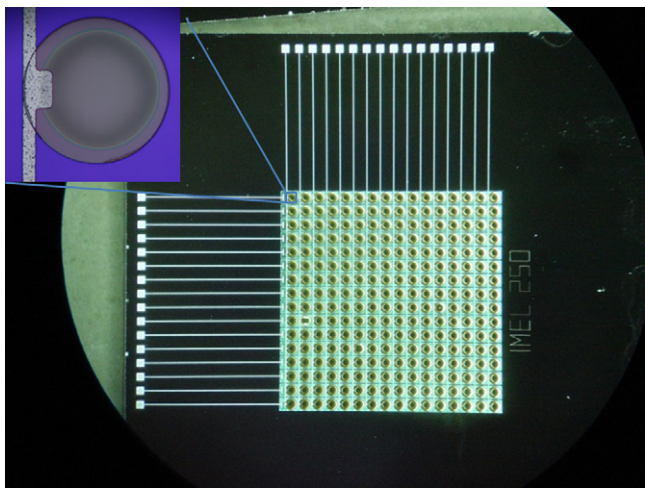
tive sensing element is depicted in Fig. 1. The capacitor plates are the flexible Si membrane that is highly boron doped in order to become conductive, and the fixed phosphor doped counter electrode. The spacing between the capacitor plates is determined by the thickness of a silicon dioxide layer that supports the membranes peripherally. A cavity etched in the SiO$_2$ layer allows for the membrane deflection. On the membrane surface, prior to testing, probe molecules are immobilized and waiting for binding with their respective target counterparts. When this happens, arising stress on the membrane surface causes the membrane to deflect, effectively changing the capacitance between the flexible electrode and the substrate.

In order to form the sensor matrix, each sensing element is aligned onto thin stripes (rows) cut out of the device layer of an SOI wafer. Aluminium (Al) lines running perpendicular to these stripes connect the sensors in the other direction (columns) as shown in Fig. 2. Each capacitor can be addressed by the corresponding column and row. A passivation low temperature oxide (LTO) layer is covering all the array area except for the Al pads. The complete 16 × 16 biosensor array die measures 12 mm × 12 mm for ease of integration with the hybridization chamber.

2.2. Sensor array fabrication

A set of biosensor arrays that vary in the sensing element dimensions have been fabricated, resulting in sensors with membrane diameter 150, 200 and 250 μm and Si membrane thickness 0.75 μm. Each membrane is supported on the SiO$_2$ cavity wall by extending over the latter with a 20 μm long rim.

The fabrication process involves silicon fusion bonding between two wafers: a silicon on insulator (SOI) wafer which will constitute the substrate and a Si wafer with a thin strain compensated epitaxial SiGeB layer, out of which the sensor membranes are formed. The boron concentration is 1.4×10^{20} cm^{-3} in order to render the epitaxial SiGeB layer conductive and enable it to function as an effective etch-stop layer in the subsequent Si wet etching. In this

Fig. 2. Image of the 16 × 16 sensing elements capacitive biosensor array. In the inset a single sensing element is depicted.

way the membranes will constitute the conductive flexible electrodes of the sensor array. The capacitors' fixed electrodes are created on the SOI film before the wafer bonding. Therefore, the SOI wafer has undergone phosphor doping and the estimated phosphor concentration in the SOI film is 2×10^{20} cm^{-3}.

Afterwards, a 0.5 μm thick wet oxide layer is grown and the sensor cavities are formed on it utilizing optical lithography and dry etching. Finally, a 200 Å thick dry oxide film covers the fixed phosphor doped electrode preventing short circuit in case a membrane touches the substrate. The SOI wafer is later bonded to the Si wafer. The latter is then lapped and wet etched until only the thin SiGeB layer remains. On this layer the membranes are patterned. In order to isolate the membranes that belong to the same column, the wet oxide and the phosphor doped area under the oxide are etched forming the stripes (rows). In this way, the buried oxide of the SOI wafer and a thin low temperature silicon oxide (LTO) layer that is deposited afterwards, isolate the neighbouring membranes along the different rows. Along each row, the membranes share the same phosphor doped stripe of the substrate. After the contacts to the substrate are opened, the Al contacts are formed. The Al lines that connect the membranes run perpendicular to the stripes and connect the sensors in the vertical direction (columns). Next, a passivation LTO layer of 0.5 μm thickness is covering all the array area except of the Al pads. The main steps of the sensor array fabrication process are described more in detail in (Tsouti et al., 2008). The immobilization of the sensing material takes place directly on the LTO layer (SiO$_2$) through the process described next.

2.3. Biological material—functionalization

2.3.1. Biological material

The DNA hybridization experiments were performed using beta-thalassemia oligonucleotides. In beta-thalassemia disease more than 200 different molecular mutations have been characterized to date. The most frequently encountered (over 90% of total mutations) molecular abnormalities are point mutations (substitutions) and short insertions or deletions limited to a few nucleotides. Among these, we selected the CD19 mutation. The CD19 is a point mutation (substitution A → G) and represents one of the most important and frequent category of mutations on beta globin gene. Nevertheless, the selection of the CD19 mutation for this study was not based on the frequency on the population but mainly on the signal intensity that we achieved in microarray genotyping experiments. Moreover, our experimental data indicated that this mutation presents a good ratio between normal and mutated allele.

Before the functionalization of the sensors, a detailed study on the surface functionalization and the immobilization of the probe oligonucleotides was performed. The oligonoucleotides contained an aminogroup at their 5′end and thus their immobilization was accomplished by functionalizing the sensor surface in order to create groups which interact with aminogroups (Manning et al., 2003).

2.3.2. Evaluation of surface functionalization and probe immobilization

In order to find the best procedure to functionalize the sensor surface and immobilize the probe molecules a series of experiments was performed using Si samples on which an LTO film (1 μm thick) was deposited so as to have the same finish as that of the sensors. During these experiments five different coating procedures were compared in order to immobilize biomolecules conjugated with amino reactive groups. The samples were coated with 3-[2-(2-Aminoethylamino)ethylamino]propyltrimethoxysilane (AEEPTMS), 3-(Aminopropyl)trimethoxysilane (APTMS), (3-Aminopropyl)tris(trimethylsiloxy)silane (APTTMS), PAMAM dendrimer (4 generation) and 3-Aminopropyltriethoxysilane (APTES). The aminogroup density offered by each type of aminosilanes was evaluated with the fluorescent dye Alexa-555-NHS. The strongest fluorescence signal was achieved with APTTMS indicating the maximum number of available aminogroups on the surface. In addition APTTMS had very low background fluorescence signal.

In order to immobilize biomaterials which contain aminogroups, on the surface of the capacitive sensor array, surface functionalization was carried out by activating the five different types of aminosilane with 1,4-Phenylene diisothiocyanate (PDITC) and gloutaldehyde, as well as coating with GOPS (3′-glucidoxypropyltrimethoxysilane).

The evaluation of the coating procedures was achieved through the immobilization of Cy3 labelled oligonucleotides which have at their 5′end an aminogroup and R-phycoerythrin streptavidin. After recording the fluorescent signal of the captured oligos and proteins, the quantity of the immobilized biomaterial as well as the quality of the coating were evaluated. Comparison, then, of the fluorescent signal yielded the optimum immobilization procedure of the oligonucleotides. In our case optimum results were achieved by coating the surface with APTTMS and activating it with PDITC.

2.3.3. Functionalization of the capacitive microarrays

Taking into account these experiments, the LTO surface of the capacitive micro-membrane arrays was functionalized by coating the array surface with APTTMS and activating it with PDITC. In particular, the functionalization process was as follows: immersion of the sample in 1% aminosilane, 95% ethanol solution for 19 h, washing twice with 95% ethanol and twice with double distilled water (ddH$_2$O) and drying with air. During the latter procedure plastic containers were used. The PDITC activation procedure was achieved by immersing the sample in 0.2% PDITC, 10% pyridine, 90% dimethylformamide (DMF) solution, washing twice with DMF and once with ethanol, and drying with air. The spotting buffer contained 3× SSC (saline sodium citrate) and 5% DMSO (dimethyl sulfoxide)—0.01% maltoside. Each spot enclosed around of 0.1 μL from oligonucleotide solution. Finally, the samples were placed in a humidity chamber at room temperature for 16 h and then dried at 80 °C for 20min.

Before the hybridization procedure, the active groups of the surface were blocked with 1% BSA (bovine serum albumin) 5× SSC 0.1 SDS for 1.5 h at 42 °C and washed five times with ddH$_2$O. On the same array, apart from the non-immobilized membranes that were used as reference, two different oligonucleotides, CD 19 normal (CD19N) and CD 19 mutated (CD19M), were immobilized on the functionalized surface of selected sensing elements. The poly-
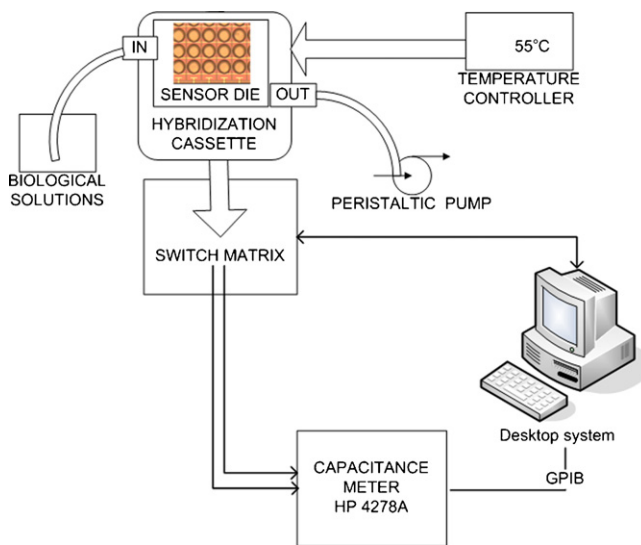
Fig. 3. Experimental setup.

merase chain reaction (PCR) product was designed to hybridize only the CD19 normal oligonucleotides.

2.4. Experimental setup

As seen in Fig. 2, the contacts to the biosensors are spaced far from the die rim in order to let enough space for a polydimethylsiloxane (PDMS) gasket to settle in and limit the bioreaction over the active area. The PDMS gasket is part of a larger enclosure, the hybridization cassette, which has been especially developed for the capacitive biosensor array and which accommodates one fluidic input and one output thus allowing for the controlled insertion of reaction fluids and necessary buffers within the limited space defined by the gasket and over the sensor array. The sensor array itself is mounted onto a printed circuit board (PCB), which provides the necessary electrical connections to the outside world and is hosted within the hybridization cassette. In order to allow for the scanning of the whole array, the PCB edge was designed to be compatible to Peripheral Component Interconnect (PCI-Express) plugging directly in a standard connector on a 16×16 switch relay matrix. Control of the whole system is performed via a Labview program running on a PC, able to control the switch matrix and an LCR bridge, and thus enabling the concurrent measurement of multiple sensors.

To operate the system, $0.5 \, \mu m$ inside diameter (ID) silicone tubing is used to implement the fluidic ways and a peristaltic pump is introduced at the exit of the microfluidic system. The pump draws the solution out of the tank and into the hybridization cassette and chamber and then out to an external waste tank. The time needed for the fluids to enter the hybridization cassette was measured during each experiment and was taken into account in order to know exactly when the solutions flow above the sensors. Finally, the temperature is controlled within $1 \, ^\circ C$ using a temperature controller and a hotplate, onto which the hybridization cassette is positioned. The experimental setup is shown in Fig. 3.

3. Results and discussion

3.1. Experimental conditions

The sensor arrays used in the experiments were composed of membrane sensing elements of $250 \, \mu m$ diameter as these were expected to be more flexible and thus more sensitive. Some sensing elements were covered with CD19N probe molecules and some with CD19M. On the remaining elements neither probe was immobilized in order for them to be used as reference. Out of the two types of the probe molecules, only CD19N are fully complementary to the target molecules. During the experiments, the capacitance values of sensing elements containing both types of probe molecules and also of reference membranes were monitored simultaneously during the hybridization process.

The hybridization experiments took place at $55 \, ^\circ C$. The hybridization temperature depends on the design of the oligonucleotides (length, GC content) and on the hybridization buffer. For this purpose, we decided to use tetramethylammonium chloride (TMAC) containing buffer which is preferred in the hybridization of oligonucleotide probes in order to eliminate the dependence of the melting temperature on the GC content of the probe, thus allowing the stringency of the hybridization to be controlled as a function of probe length only. Our experimental data based on spotted LTO/Si substrates indicated that the efficiency of the hybridization is higher when performed at $55 \, ^\circ C$. Therefore, the hybridization experiments using the capacitive micro-membrane arrays included the sequential insertion into the hybridization chamber of the following solutions: (1) TMAC buffer; (2) double distilled water (ddH_2O); (3) the PCR product of the complementary to CD19N strands, which remained into the chamber for several hours; and (4) TMAC buffer in order to wash away the non-specifically bound molecules.

3.2. Response of the biosensor array

In a typical experiment, the sensor capacitance acquires at first a stable value during TMAC washing. Then, during washing with water, the sensor capacitance falls and remains stable until the PCR product is inserted in the hybridization chamber. At this time and until the oligonucleotide hybridization begins to take place, the sensor capacitance remains stable thus creating a plateau in the sensor response curve. This plateau is then taken as a baseline for the monitoring of the DNA hybridization. The hybridization event becomes evident as a slow decrease in the sensor capacitance before coming to a new stable value again. The baseline itself can then be used to normalize the responses of the sensors to a common reference.

In Fig. 4 a typical result is depicted. The CD19 probe molecule concentration was $100 \, \mu M$ and the PCR product concentration $5.26 \times 10^{-3} \, g/L$ or $72 \, nM$. In Fig. 4 the response curves of several sensors after obtaining the baseline are depicted. As shown, after the PCR insertion, the sensors signals remain stable at first and then decrease for both mutated and normal sensors as well as the references. However the decrease in the normal CD19 is by far larger than the other two, an indication that a hybridization reaction is taking place between the immobilized CD19N probes on the surface of the sensor and the PCR solution under analysis. The spread in the individual sensor response is attributed to localized residual mechanical stress across the wafer and across the biosensor array die (the die is quite large). These, in turn, are dependent on deposition conditions of the various constructing layers (SiGeB, LTO, Al). LTO in particular has been known to suffer from stresses as high as $400 \, MPa$. Other sources of residual stresses which influence device response and thus contribute to the spread of each individual sensor response include the substrate wafer thickness and flatness variations as well as the overall wafer bow and warp.

The mutated CD19 probe oligonucleotides, which have a single nucleotide mismatch in their sequence, show very little response. On the contrary, the average differential signal of normal CD19 sensors is about $13 \, pF$, whereas the average initial capacitance value of the sensors is $65 \, pF$. The capacitance decrease, translated as the capacitor plates' deflection, indicates upward deflection of the
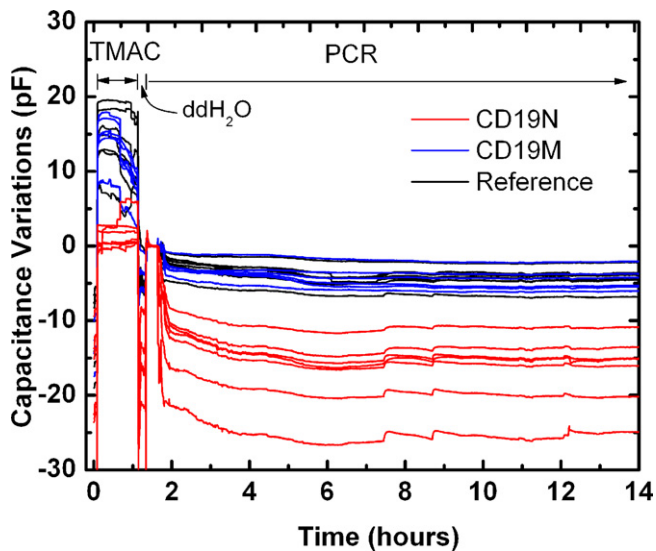
Fig. 4. Typical response of the biosensor array during the hybridization experiments. The functionalized with the fully complementary to PCR product sensors (CD19N) show significant capacitance decrease compared to the single nucleotide mismatched (CD19M) and reference sensors.
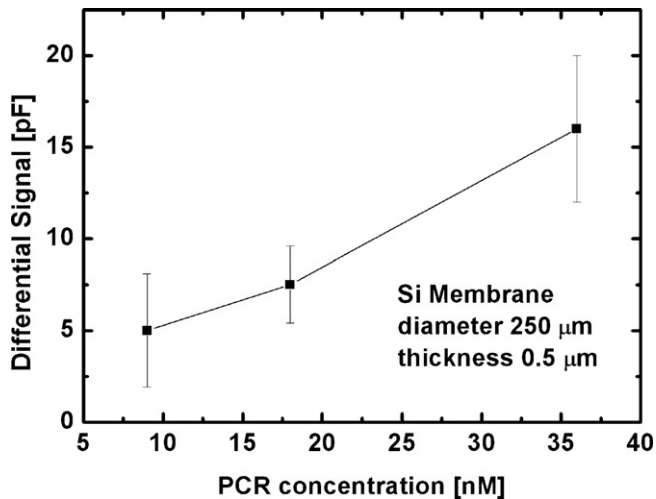

Fig. 5. Average differential response (average CD19N minus average CD19M sensors) of biosensor arrays with sensing elements of 0.5 μm Si membrane thickness and 250 μm diameter for three different PCR concentrations. The errors are estimated by the variations among the sensing elements in the same array.

membranes and thus a compressive surface stress increase during the hybridization event. This result is in agreement with the reported surface stress variations in cantilevers (Fritz et al., 2000; Zhang et al., 2006) as well as in polymer membranes (Cha et al., 2008).

In Fig. 5 the response of the array to three different PCR product concentrations (9, 18 and 36 nM) is depicted. In this case a different sensor batch with thinner (0.5 μm), more sensitive membranes, was used. The estimated *y*-axis error, in the graph, is obtained by the standard deviation of the sensors' capacitance changes in the array.

4. Conclusion

We demonstrated the capacitive detection of DNA hybridization using a Si micromechanical biosensor array. The deflection variations of the ultrathin Si membranes are transformed into capacitance changes between the membrane and the substrate. Experiments using fully complementary as well as single base mismatched beta-thalassemia DNA strands showed that the surface stress variations that occur during the hybridization of oligonucleotides are able to cause changes in the deflection of Si membranes that are part of the developed array. The sensors are able to discriminate between a fully complementary sequence and a single nucleotide mismatch, indicating that they have a potential for reliable detection of decease related mutations. The capacitive biosensor array allows for the direct, fast and real-time study of the biological interactions. The capacitance technique is very simple, resulting in simplification of the experimental procedure and the potential fabrication of systems of low cost and small size, thus suitable for point of care applications. Moreover, the array die size may be further miniaturized, by using sensors with thinner and smaller diameter. However, its overall size is mainly determined by the microfluidic connections necessary to move the solutions around. To this end, future work will focus in the integration of the hybridization chamber on chip.

References

Benini, L., Paulus, C., Guiducci, C., 2007. Biochips. IEEE Des. Test Comput. 2007 (January–February), 38–48.
Berggren, C., Bjarnason, B., Johansson, G., 2001. Electroanalysis 13, 173–180.
Bhanot, G., Louzoun, Y., Zhu, J., DeLisi, C., 2003. Biophys. J. 84, 124–135.
Cha, M., Shin, J., Kim, J.-H., Kim, I., Choi, J., Lee, N., Kim, B.-G., Lee, J., 2008. Lab Chip 8, 932–937.
Chen, X., Sullivan, P.F., 2003. Pharmacogenomics J. 3, 77–96.
Dai, H., Meyer, M., Stepaniants, S., Ziman, M., Stoughton, R., 2002. Nucl. Acids Res. 30, e86.
Daniels, J.S., Pourmand, N., 2007. Electroanalysis 19, 1239–1257.
Fritz, J., Baller, M.K., Lang, H.P., Rothuizen, H., Vettiger, P., Meyer, E., Güntherodt, H.J., Gerber, Ch., Gimzewski, J.K., 2000. Science 288, 316–318.
Fritz, J., 2008. Analyst 133, 855–863.
Guiducci, C., Stagni, C., Fischetti, A., Mastromatteo, U., Benini, L., Riccò, B., 2006. IEEE Sensors J. 6, 1084–1093.
Hansen, K.M., Ji, H.-F., Wu, G., Datar, R., Cote, R., Majumdar, A., Thundat, T., 2001. Anal. Chem. 73, 1567–1571.
Levine, P.M., Gong, P., Levicky, R., Shepard, K.L., 2009. Biosens. Bioelectron. 24, 1995–2001.
Manning, M., Harvey, S., Galvin, P., Redmond, G., 2003. Mater. Sci. Eng. C 23, 347–351.
Mehta, M., Hanumanthaiah, C.S., Betala, P.A., Zhang, H., Roh, S.W., Buttner, W., Penrose, W.R., Stetter, J.R., Pérez-Luna, V.H., 2007. Biosens. Bioelectron. 23, 728–734.
Mukhopadhyay, R., Lorentzen, M., Kjems, J., Besenbacher, F., 2005. Langmuir 21, 8400–8408.
Park, K.K., Lee, H.J., Yaralioglu, G.G., Ergun, A.S., Oralkan, Ö., Kupnic, M., Quate, C.F., Khuri-Yakub, B.T., Braun, T., Ramseyer, J.-P., Lang, H.P., Hegner, M., Gerber, Ch., Gimzewski, J.K., 2007. Appl. Phys. Lett. 91, 094102.
Peterson, A.W., Heaton, R.J., Georgiadis, R.M., 2001. Nucl. Acids Res. 29, 5163–5168.
Satyanarayana, S., McCormick, D.T., Majumdar, A., 2006. Sens. Actuators B 115, 494–502.
Shiu, S.-H., Borevitz, J.O., 2008. Heredity 100, 141–149.
Sivaramakrishnan, S., Rajamani, R., Pappenfus, T.M., 2008. Sens. Actuators B 135, 262–267.
Tsouti, V., Chatzandroulis, S., Goustouridis, D., Normand, P., Tsoukalas, D., 2008. Microelectron. Eng. 85, 1359–1361.
Tsouti, V., Boutopoulos, C., Andreakou, P., Ioannou, M., Zergioti, I., Goustouridis, D., Kafetzopoulos, D., Tsoukalas, D., Normand, P., Chatzandroulis, S., 2009. Microelectron. Eng. 86, 1495–1498.
Zhang, J., Lang, H.P., Huber, F., Bietsch, A., Grange, W., Certa, U., McKendry, R., Güntherodt, H.-J., Hegner, M., Gerber, Ch., 2006. Nat. Nanotechnol. 1, 214–220.